JOURNAL OF MATERIALS SCIENCE 18 (1983) 3712–3720

Fracture mechanisms in microstrength testing of carbon artifacts

S. RAGAN*, H. MARSH
Northern Carbon Research Laboratories, School of Chemistry, University of Newcastle upon Tyne, Newcastle upon Tyne, UK

Failure mechanisms in baked carbons prepared from oxidized needle-coke and a coal-tar pitch binder are examined in terms of their optical texture and microstrength. Models are presented which describe interfaces between binder coke and filler coke and the failure mechanisms at these interfaces. Crack growth can occur at the interface between binder and filler; crack growth can interconnect the fissured interfaces between oxidized filler coke and binder; crack growth can occur between binder and filler cokes across a wetted/keyed interface.

1. Introduction

A previous publication of Ragan and Marsh [1] considers the use of oxidized needle-cokes in the preparation of carbon artifacts. The nature of interactions between pitch, pitch-coke and filler coke directly influences the strength (microstrength) of resultant artifacts. This paper attempts to examine the failure mechnisms exhibited by the artifacts described earlier [1]. It considers the influence of interactions between pitch-coke (binder-coke) and filler coke upon micro-crack behaviour. Similar studies based on the behaviour of coal derived cokes have also been published [2, 3].

This paper therefore examines the microstrength, optical texture and failure mechanisms in baked carbons resulting from the use of oxidized needle-coke and a pitch binder. Attention is directed especially to an optical microscopy examination of the coke fragments following microstrength testing in an attempt to ascertain mechanisms of failure.

2. Experimental details

The artifacts used are described [1]. Microstrength testing has also been fully described [4]. The sieve fractions from the microstrength testing of the artifacts [1] were retained for examination by optical microscopy. The sized product, $> 600\,\mu m$, was mounted in polyester resin and polished. Optical texture and crack behaviour were examined and photographed in reflected, polarized light using a Vickers M17 Photoplan Microscope as described [1].

3. Results

3.1. Optical microscopy

Fig. 1 shows the optical texture of a carbon artifact from calcined Conoco needle-coke with 35% BSC No. 2 electrode binder pitch after microstrength testing. Position A shows microcrack propagation preferentially at the interface between the filler and binder coke.

Fig. 2 shows the optical texture of a carbon artifact from Conoco needle-coke (5% oxidized) with 35% BSC No. 2 electrode binder pitch after microstrength testing. Position B shows a microcrack moving into and exploiting the fissured interface between the binder and filler cokes.

Fig. 3 shows the optical texture of a carbon artifact from Conoco needle-coke (10% oxidized) with 35% BSC No. 2 electrode binder pitch after microstrength testing. Position C shows microcrack propagation through the binder into the filler coke across the interface.

Fig. 4 shows the optical texture of a carbon artifact from Conoco needle-coke (20% oxidized) with 35% BSC No. 2 electrode binder pitch after

*Present address: Petro-Canada, Process Research Laboratories, PO Box 2844, Calgary, Alberta T2P 3E3, Canada.

0022–2461/83 $03.00 + .12

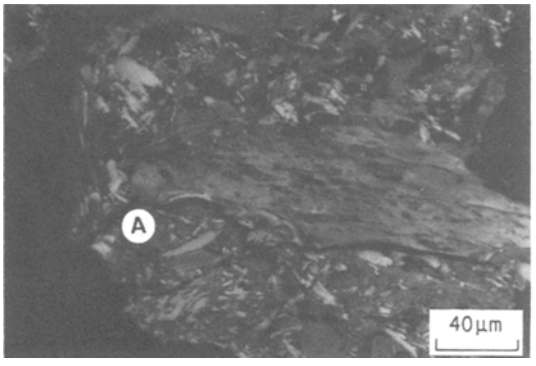

Figure 1 Optical micrograph of carbon artifact from Conoco needle-coke with 35% BSC No. 2 electrode binder pitch. After microstrength testing. HTT 1273 K, 4 K min^{-1}, in nitrogen. Position A shows microcrack propagation through the binder coke then preferentially along the interface with the filler.

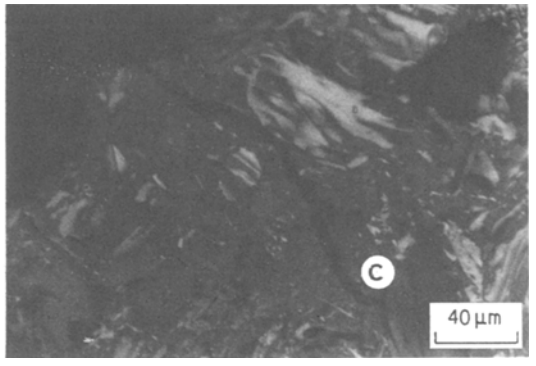

Figure 3 Optical micrograph of carbon artifact from Conoco needle-coke (10% oxidized) with 35% BSC No. 2 electrode binder pitch. After microstrength testing. HTT 1273 K, 4 K min^{-1}, in nitrogen. Position C shows microcrack propagation from the binder into the filler coke.

microstrength testing. Position D shows microcrack development in the filler coke.

Fig. 5 shows the optical texture of a carbon artifact from calcined Shell needle-coke with 35% BSC No. 2 electrode binder pitch after microstrength testing. Position E shows microcrack propagation along the interface between the filler and binder cokes.

Fig. 6 shows the optical texture of a carbon artifact from Shell needle-coke (5% oxidized) with 35% BSC No. 2 electrode binder pitch after microstrength testing. Position F shows microcrack propagation along the interfaces of two particles of binder and filler coke.

Fig. 7 shows the optical texture of a carbon artifact from Shell needle-coke (10% oxidized) with 35% BSC No. 2 electrode binder pitch after microstrength testing. Position G shows microcracks interconnecting the fissured interfaces between binder and filler coke.

Fig. 8 shows the optical texture of a carbon artifact from Shell needle-coke (20% oxidized) with 35% BSC No. 2 electrode binder pitch after microstrength testing. Position H shows microcrack propagation from the binder coke to the interface with filler coke and continuing along the surface.

Fig. 9 shows the optical texture of an artifact from an NCB calcined coal extract coke No. 18 with 35% BSC No. 2 electrode binder pitch after microstrength testing. Position J shows microcracks interconnecting fissured interfaces between the binder and filler cokes.

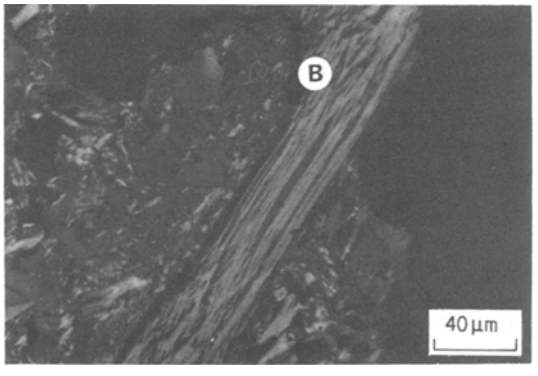

Figure 2 Optical micrograph of carbon artifact from Conoco needle-coke coke (5% oxidized) with 35% BSC No. 2 electrode binder pitch. After microstrength testing. HTT 1273 K, 4 K min^{-1}, in nitrogen. Position B shows a microcrack exploiting the fissured interface.

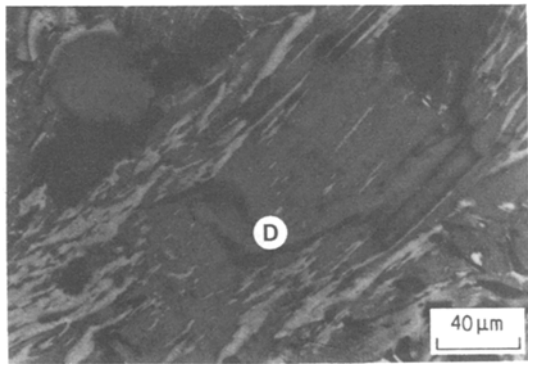

Figure 4 Optical micrograph of carbon artifact from Conoco needle-coke (20% oxidized) with 35% BSC No. 2 electrode binder pitch. After microstrength testing. HTT 1273 K, 4 K min^{-1}, in nitrogen. Position D shows microcrack growth in the filler.

Figure 5 Optical micrograph of carbon artifact from Shell needle-coke with 35% BSC No. 2 electrode binder pitch. After microstrength testing. HTT 1273 K, 4 K min^{-1}, in nitrogen. Position E shows microcrack propagation at the interface between the filler (needle-coke) and binder coke.

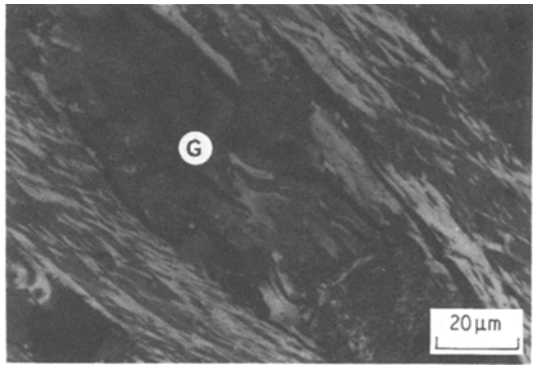

Figure 7 Optical micrograph of carbon artifact from Shell needle-coke (10% oxidized) with 35% BSC No. 2 electrode binder pitch. After microstrength testing. HTT 1273 K, 4 K min^{-1}, in nitrogen. Position G shows microcracks interconnecting the fissured interfaces of the filler and binder coke.

Fig. 10 shows the optical texture of an artifact from an NCB coal extract coke No. 18 (5% oxidized) with 35% BSC No. 2 electrode binder pitch after microstrength testing. Position K shows crack growth at the interface between binder and filler cokes with considerable subsiduary microcracking in the binder coke.

Fig. 11 shows the optical texture of an artifact from an NCB coal extract coke No. 18 (10% oxidized) with 35% BSC No. 2 electrode binder pitch after microstrength testing. Position L shows crack propagation from the binder coke through the filler coke across the interface between the two cokes.

Fig. 12 shows the optical texture of an artifact from an NCB coal extract coke No. 18 (20% oxidized) with 35% BSC No. 2 electrode binder pitch after microstrength testing. Position M shows microcrack growth in the filler coke.

Fig. 13 shows optical texture of an artifact from an NCB coal extract coke No. 18 (20% oxidized) with 35% BSC No. 2 electrode binder pitch after microstrength testing. Positions N and O show microcrack propagation at interfaces between binder and filler cokes.

3.2. Models of interface structure

Fig. 14 shows idealized models of the types of interface developed by needle-coke fillers with binder coke [1]. Fig. 14a, shows a wetted interface

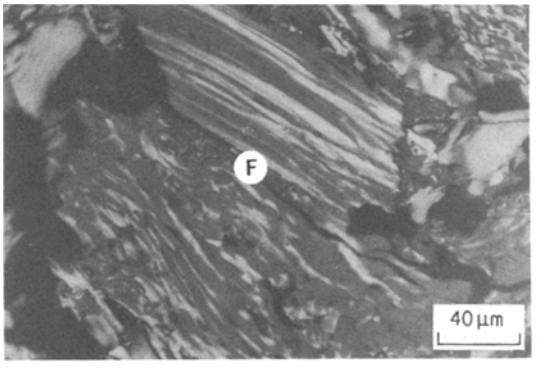

Figure 6 Optical micrograph of carbon artifact from Shell needle-coke (5% oxidized) with 35% BSC No. 2 electrode binder pitch. After microstrength testing. HTT 1273 K, 4 K min^{-1}, in nitrogen. Position F shows microcrack propagation at the interface between the filler and binder coke.

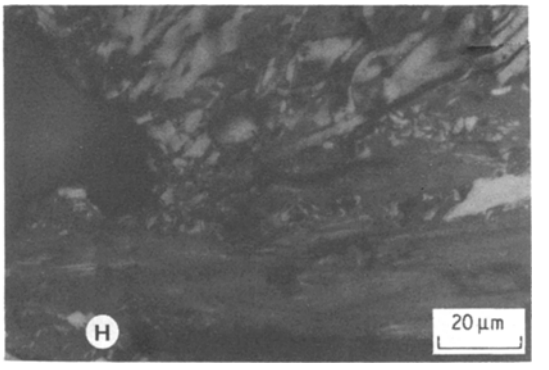

Figure 8 Optical micrograph of carbon artifact from Shell needle-coke (20% oxidized) with 35% BSC No. 2 electrode binder pitch. After microstrength testing. HTT 1273 K, 4 K min^{-1}, in nitrogen. Position H shows microcrack propagation from binder coke, along interface between filler and binder cokes.

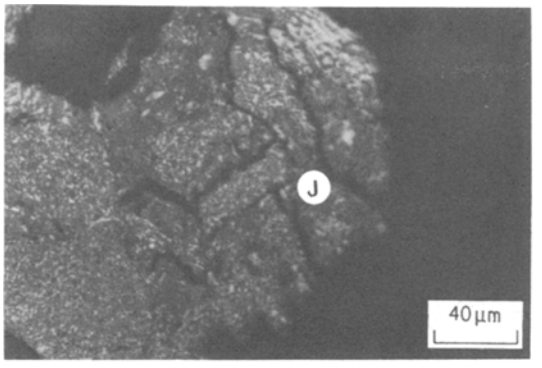

Figure 9 Optical micrograph of carbon artifact from NCB coal extract coke No. 18 with 35% BSC No. 2 electrode binder pitch. After microstrength testing. HTT 1273 K, 4 K min^{-1}, in nitrogen. Position J shows microcracks interconnecting fissured interfaces between filler and binder components.

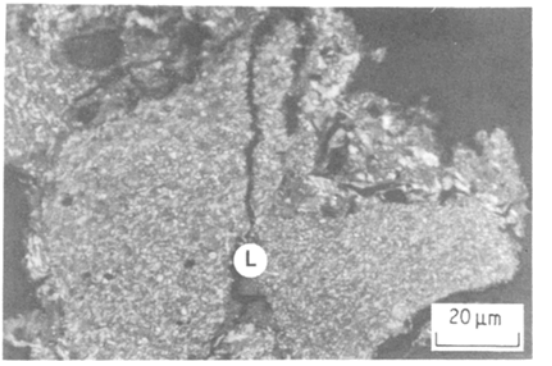

Figure 11 Optical micrograph of carbon artifact from NCB coal extract coke No. 18 (10% oxidized) with 35% BSC No. 2 electrode binder pitch. After microstrength testing. HTT 1273 K, 4 K min^{-1}, in nitrogen. Position L shows microcrack propagation from binder into filler across the interface between the two cokes.

typical of the non-oxidized binder/filler interactions in artifacts containing needle-coke fillers. Fig. 14b shows the fissured interface, typical of partially oxidized binder/filler interactions and Fig. 14c shows the wetted/keyed interface where surface features, e.g. pits developed on the filler particles as a result of extensive oxidation have been penetrated and wetted by the binder pitch.

Fig. 15 shows idealized models of the fracture mechanism of artifacts containing needle-coke fillers, as a result of microstrength testing, relative to the types of interface developed between the binder and filler cokes. Fig. 15a shows crack growth at the interface between filler and binder, i.e. typical fracture mechanism in all of the artifacts examined. Fig. 15b shows crack growth interconnecting the fissured interfaces between oxidized filler and binder, a common fracture mechanism in artifacts containing oxidized needle-coke fillers, i.e. Fig. 7, Position G. Fig. 15c shows crack growth between the binder and filler cokes across a wetted/keyed interface. This type of fracture mechanism is only seen in artifacts containing heavily oxidized needle-coke fillers, i.e. 20% oxidation, Fig. 4, Position D.

Fig. 16 shows idealized models of the types of interfaces developed by a coal extract coke No. 18 filler with binder coke [1]. Fig. 16a shows the fissured interface typical of the non-oxidized and 5% oxidized coal extract coke fillers with binder coke. Fig. 16b shows the wetted/keyed interface

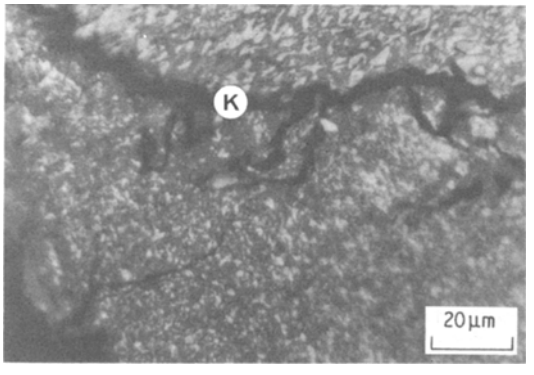

Figure 10 Optical micrograph of carbon artifacts from NCB coal extract coke No. 18 (5% oxidized) with 35% BSC No. 2 electrode binder pitch. After microstrength testing. HTT 1273 K, 4 K min^{-1}, in nitrogen. Position K shows microcrack growth at interface between filler and binder cokes with subsidiary cracking in the binder.

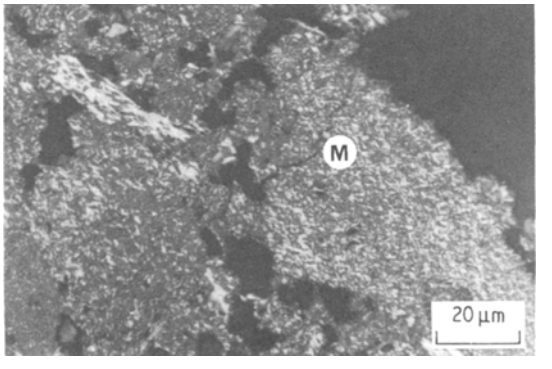

Figure 12 Optical micrograph of carbon artifact from NCB coal extract coke No. 18 (20% oxidized) with 35% BSC No. 2 electrode binder pitch. After microstrength testing. HTT 1273 K, 4 K min^{-1}, in nitrogen. Position M shows microcrack growth in filler coke.

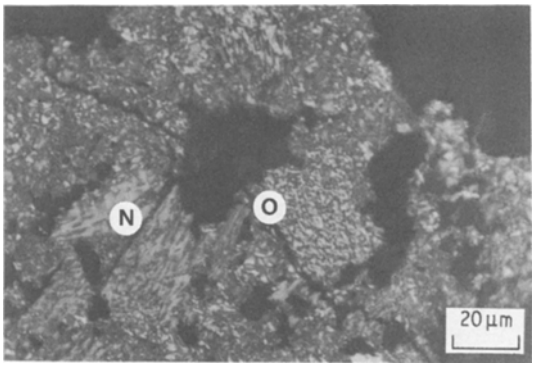

Figure 13 Optical micrograph of carbon artifact from NCB coal extract coke No. 18 (20% oxidized) with 35% BSC No. 2 electrode binder pitch. After microstrength testing. HTT 1273 K, 4 K min^{-1}, in nitrogen. Positions N and O show microcrack propagation at interfaces between filler and binder cokes.

typical of the filler/binder interaction in artifacts containing 10 to 20% oxidized coal extract coke filler.

Fig. 17 shows idealized models of the fracture mechanisms shown by artifacts containing coal extract coke following microstrength testing and related to the type of interface developed between the filler and binder cokes. Fig. 17a shows crack growth interconnecting the fissured interfaces between binder and filler cokes, this being a common mechanism in artifacts containing non-oxidized and 5% oxidized extract coke fillers, i.e. Fig. 9, Position J. Fig. 17b shows crack growth between binder and filler cokes across a keyed interface, i.e. a common mechanism in artifacts containing oxidized extract coke filler, i.e. 10 to 20% oxidation, Figs. 11, 12, Positions L and M.

4. Discussion

Examination of the fracture behaviour resulting from microstrength testing in artifacts containing needle-coke fillers indicates that the type of interface developed between the binder and filler cokes largely controls microcrack formation and growth and hence the microstrength of the artifact.

4.1. Needle-cokes

In all the artifacts the typical fracture mechanism is that of microcrack growth at the interface between binder and filler coke Fig. 15a. Hence, changes in the type of interface, resulting from oxidation of the filler, have a marked influence on the microstrength of the artifact. Ragan and Marsh [1] show for non-oxidized needle-coke fillers that the filler particles were "wetted" by the molten binder pitch during mixing this resulting in a close, but discontinuous, contact between the binder and filler This contact between the binder and filler is maintained during con-

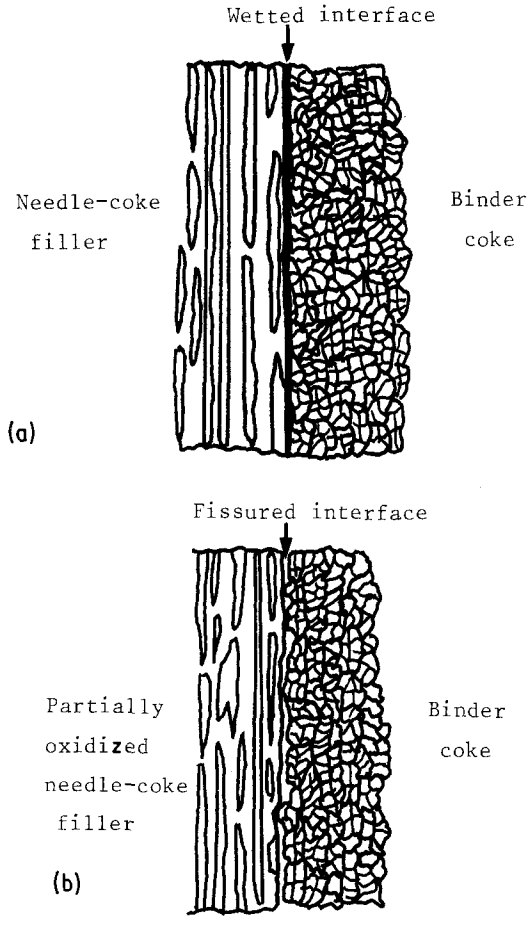

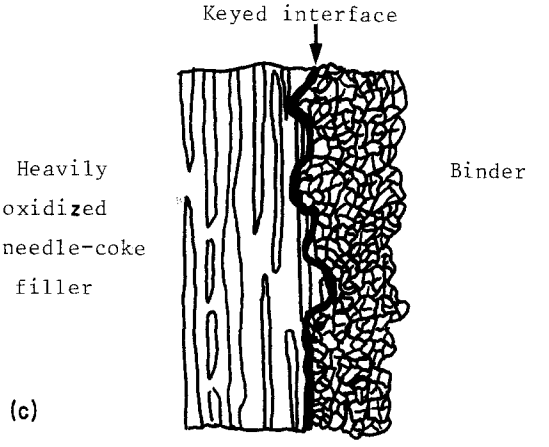

Figure 14 Models of the type of interfaces observed between needle-coke fillers and binder coke; (a) wetted interface, (b) fissued interface, (c) keyed interface.

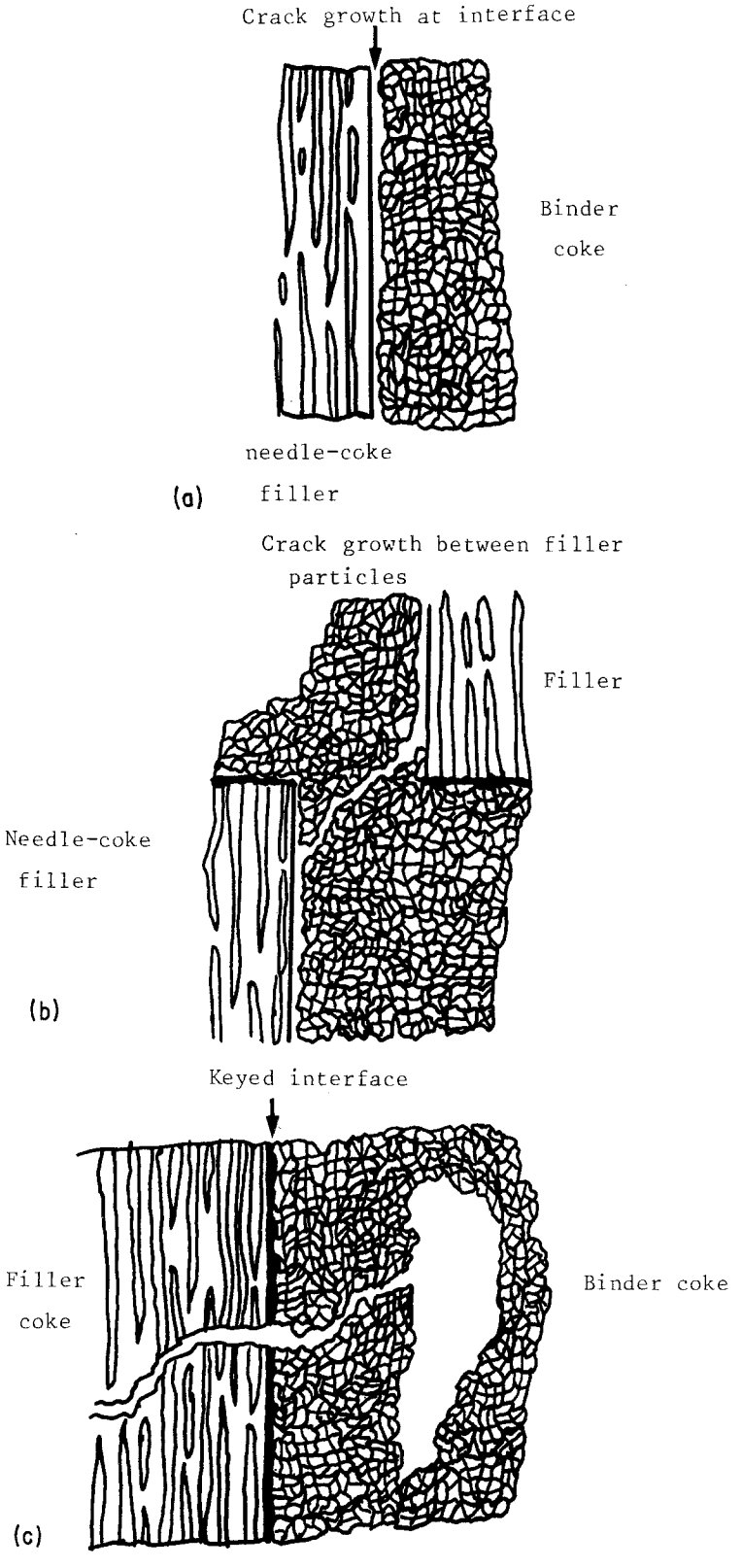

Figure 15 Models of observed crack growth in artifacts made with needle-coke filler; (a) growth at interface; (b) growth connecting interfaces; (c) growth across the interface.

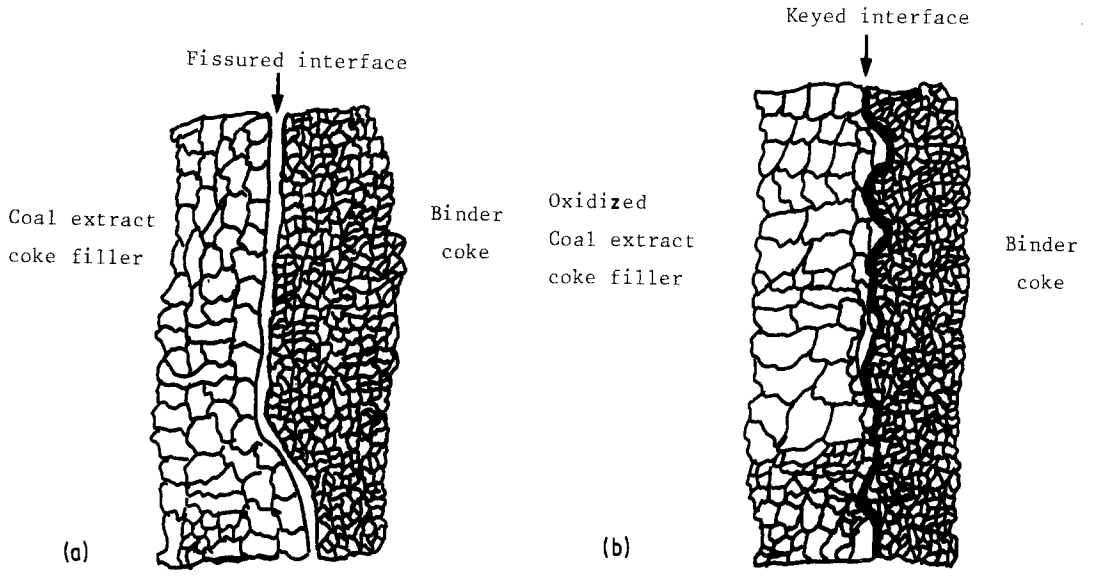

Figure 16 Models of the types of interfaces observed between coal extract filler and binder coke; (a) fissured interface; (b) keyed interface.

traction of the binder, on baking, resulting in a distinct "wetted" interface between the binder and filler cokes. Microcrack growth at these interfaces, resulting from stress in the artifact induced by microstrength testing, results from propagation of the discontinuity existing between the binder and filler coke at the wetted surface. The formation of fissures at the interface between binder coke and oxidized needle-coke filler is shown in Fig. 14. Pits developed in the surface of the filler particles, as a result of oxidation, inhibit the wetting interaction between binder and filler by being too small to be penetrated by the molten binder, i.e. $< 4\,\mu m$. This results in reduced contact between the binder and filler coke and the development of fissures at the interface results from contraction of the binder on baking. The development of this type of interface markedly reduces the microstrength of resultant artifacts. Crack growth at the interface between filler and binder (Fig. 15a) is facilitated by pre-existing interfacial fissures. Microcracks grow through the interconnecting fissured interfaces (Fig. 15b). This combination of failure mechanisms results in the marked decline in the microstrength of the artifacts [1].

With extensive oxidation ~20% the pits on the surface of the filler particles become of sufficient size, i.e. $> \sim 5\,\mu m$ to be penetrated by the molten binder pitch producing a wetted, keyed, interface, i.e. Fig. 14c. This results in an improved bonding between the binder and filler cokes, but has little effect on the strength of resultant artifacts as the strength of the needle-coke filler itself deteriorates markedly with increasing oxidation [1]. Hence, stresses in the artifact, from the microstrength testing, produce microcracks which will easily propagate from the binder, into and through the filler particles (Fig. 15c) counteracting any improvement in artifact strength resulting from enhanced bonding.

4.2. Coal extract coke

Fracture mechanisms found in microstrength testing in artifacts containing coal extract filler coke again indicate that the type of interface developed between the binder and filler cokes largely controls microcrack formation and growth and hence the micrograph of the artifact.

Generally, microcrack growth leading to failure of artifacts containing coal extract coke occurs, as with needle-cokes, preferentially at the interface between the binder and filler cokes, e.g. Fig. 13, Positions N and O. However, the change from a fissured interface, Fig. 16a, to a wetted/keyed interface, Fig. 16b, resulting from oxidation of the filler, has a marked influence on the strength of the resultant artifact.

For the non-oxidized and partially oxidized (~5%) coal extract coke a fissured interface exists between the binder and filler cokes. This results from differential contraction of binder and filler

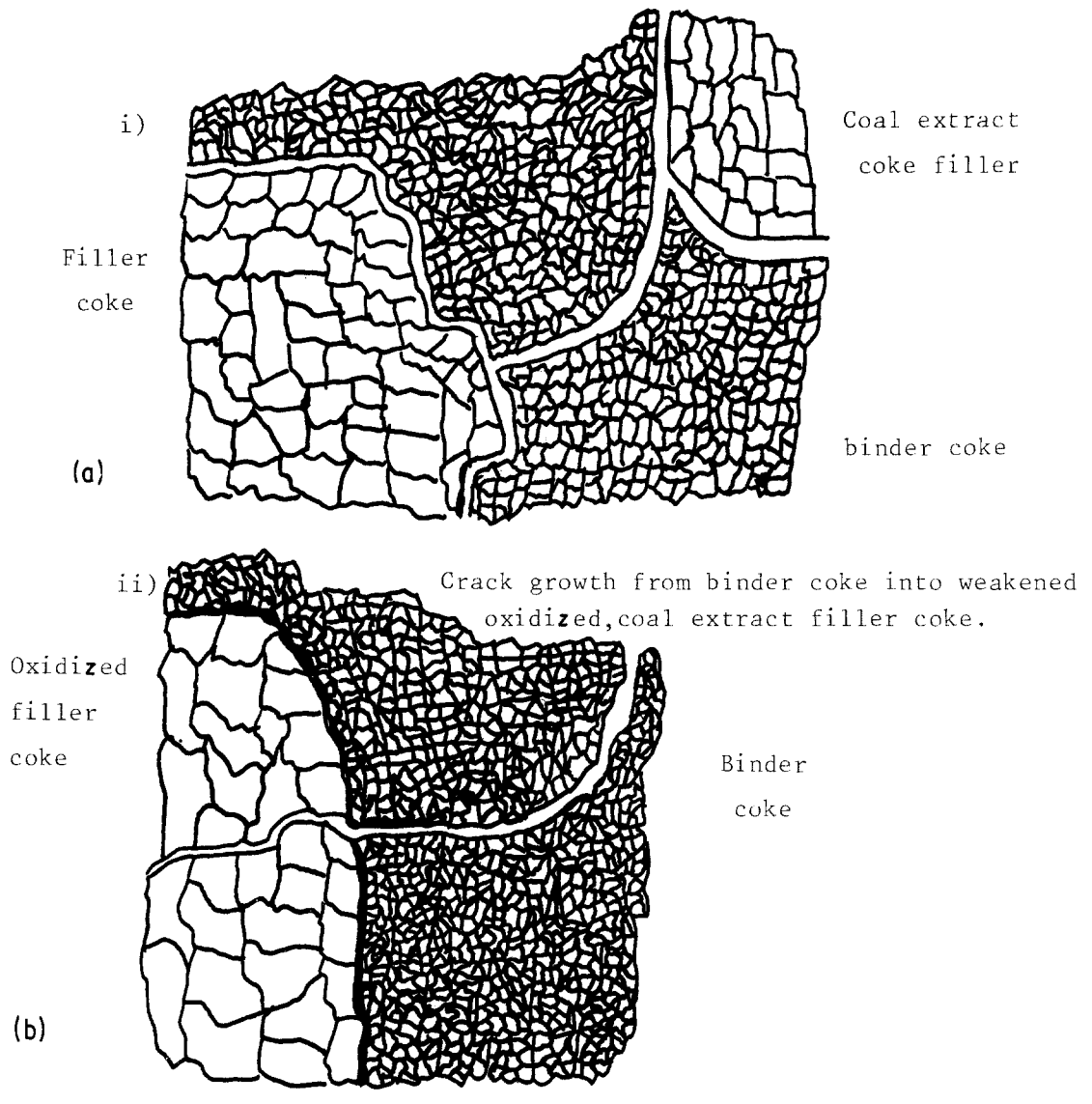

Figure 17 Models of observed crack growth in artifacts made with coal extract coke filler; (a) growth connecting interfaces; (b) growth across the interface.

cokes, during baking [1]. The fissuring at the interface between the binder and the coal extract cokes produces crack behaviour similar to that seen with oxidized needle-coke fillers. Here interfacial crack growth is facilitated by the presence of pre-existing cracks and by crack growth in binder coke through interconnecting fissured binder/filler interfaces, e.g. Fig. 17a. This combination of failure mechanisms produces relatively weak artifacts containing coal extract filler coke.

However, coal extract filler coke oxidized in the range 10 to 20% develops a wetted/keyed interface with the binder during mixing and the interface is maintained after baking. Formation of this type of interface results from the pits developed on the surfaces of the filler particles because of oxidation being large enough to allow penetration by the molten binder pitch, i.e. $> \sim 5\,\mu m$. The increased contact between the binder and filler improves mechanical interaction and prevents fissuring caused by differential contraction of the filler and binder cokes during baking. The

increased contact between the cokes resists microcrack growth at interfaces and fracture from binder coke through to the filler coke becomes prevalent, Fig. 11 Position K and Fig. 17b.

The propagation of microcracks from binder coke into and through filler coke indicates good stress transmission across the wetted/keyed interface. Where this occurs with oxidized needle-coke filler, the low strength of the oxidized filler results in a weak artifact. However, it is shown [1] that the strength of the coal extract filler coke is only marginally reduced by oxidation, internal oxidation of the coal extract coke filler being minimized by its low porosity. The high strength of the oxidized coal extract filler coke resists microcrack propagation from the binder and results in the continued strength of artifacts containing heavily oxidized coal extract filler coke, i.e. 20% oxidation.

Acknowledgements

The authors acknowledge the Koninklijke/Shell-Laboratory Amsterdam, for the supply of the needle-coke used in the research. S. R. thanks the Wolfson Foundation whose financial support made this work possible. The assistance of Miss B. A. Clow in the preparation of the manuscript is appreciated.

References

1. S. RAGAN and H. MARSH, *J. Mater. Sci.* **18** (1983) 3705.
2. *Idem, Fuel* **60** (1981) 522.
3. S. RAGAN, A. GRINT and H. MARSH, *ibid.* **60** (1981) 646.
4. S. RAGAN and H. MARSH, *J. Mater. Sci.* **18** (1983) 3695.

Received 21 March
and accepted 30 March 1983